Earthquakes and Structures, *Vol. 15, No. 2 (2018) 113-122*
DOI: https://doi.org/10.12989/eas.2018.15.2.113

Nonlinear analysis of damaged RC beams strengthened with glass fiber reinforced polymer plate under symmetric loads

Rabahi Abderezak[1,2], Tahar Hassaine Daouadji[*1,2], Benferhat Rabia[1,2] and Adim Belkacem[2,3]

[1]*Département de Génie Civil, Université Ibn Khaldoun Tiaret; BP 78 Zaaroura, Tiaret, Algérie*
[2]*Laboratoire de Géomatique et Développement Durable, Université de Tiaret, Algérie*
[3]*Département des Sciences et Technologies, Centre Universitaire Tissemsilt, Algérie*

(Received March 13, 2018, Revised April 11, 2018, Accepted April 12, 2018)

Abstract. This study presents a new beam-column model comprising material nonlinearity and joint flexibility to predict the nonlinear response of reinforced concrete structures. The nonlinear behavior of connections has an outstanding role on the nonlinear response of reinforced concrete structures. In presented research, the joint flexibility is considered applying a rotational spring at each end of the member. To derive the moment-rotation behavior of beam-column connections, the relative rotations produced by the relative slip of flexural reinforcement in the joint and the flexural cracking of the beam end are taken into consideration. Furthermore, the considered spread plasticity model, unlike the previous models that have been developed based on the linear moment distribution subjected to lateral loads includes both lateral and gravity load effects, simultaneously. To confirm the accuracy of the proposed methodology, a simply-supported test beam and three reinforced concrete frames are considered. Pushover and nonlinear dynamic analysis of three numerical examples are performed. In these examples the nonlinear behavior of connections and the material nonlinearity using the proposed methodology and also linear flexibility model with different number of elements for each member and fiber based distributed plasticity model with different number of integration points are simulated. Comparing the results of the proposed methodology with those of the aforementioned models describes that suggested model that only uses one element for each member can appropriately estimate the nonlinear behavior of reinforced concrete structures.

Keywords: material nonlinearity; joint flexibility; spread plasticity; lateral load; gravity load

1. Introduction

The rehabilitation or strengthening of reinforced concrete structures is an important problem in civil engineering. In the last few years, GFRP composites are being used in the construction industry in the form of laminates and pultruded plates for strengthening of existing structures Meier (1995). With their excellent properties such as high tensile strength, long-term durability, corrosion/fire resistance and low weight, FGRPs have almost completely replaced steel plates as externally epoxy-bonded reinforcement for concrete. An important failure mode for such members is the debonding of the FRP plate from the member because of high interfacial stresses near the plate ends. Accurate predictions of the interfacial stresses are thus important for designing against debonding failures. This technique has been widely investigated, and several examples of existing structures retrofitted using CFRP bonded composite materials can be found in the literature Tounsi (2008), Benyoucef (2006), Roberts (1989), Smith and teng (2001), Shen (2001), Yang (2007), Bouakaz (2014). Among these materials, carbon fiber polymers are extensively used because of their un paralleled characteristics Roberts (1989), Roberts and Haji-Kazemi (1989). The transferring of stresses from concrete to the FRP reinforcement is central to the reinforcement effect of FRP-strengthened concrete structures. This is because the stresses are susceptible to cause the undesirable premature and brittle failure, such as debonding of the soffit plate from the RC beam. It is therefore important to understand the mechanism of this debonding failure mode and develop sound design rules. This brittle mode of failure is a result of the high shear stress concentrations arising at the edges of the bonded FRP strip. Hence, this limited area in the close vicinity of the bonded strip edge, subjected to high peeling and interfacial shear stresses, proves to be among the most critical parts of the strengthened beam. Consequently, the determination of interfacial stresses has been researched for the last decade for beams bonded with either steel or advanced composite materials. In particular, several closed-form analytical solutions have been developed Al-Emrani (2006), Hassaine Daouadji (2016), Asharaful (2018), Awad jadooe (2018), Fu (2018), Tounsi (2008), Rabahi (2018), Rabahi (2016), Hassaine Daouadji (2016), El Mahi (2014), Guenaneche (2014), Kongjian (2018), Wensu (2018), Krour (2014), Touati (2015), Yang *et al.* (2018), Zidani (2015), Yang and Ye (2010). All these solutions are for linear elastic materials and employ the same key assumption that the adhesive is subject to shear stresses that are constant across the thickness of the adhesive layer. It is this key assumption that enables relatively simple closed-form solutions to be obtained. In the existing solutions, two different approaches

∗Corresponding author, Professor
E-mail: daouadjitahar@gmail.com

ISSN: 2092-7614 (Print), 2092-7622 (Online)

have been employed. Roberts (1989), Roberts and Haji-Kazemi (1989) used a staged analysis approach, while Vilnay (1988), Benyoucef *et al.* (2006), Smith and Teng (2001) considered directly deformation compatibility conditions.

The main objective of the present study is to analyze the interfacial shear stress in damaged RC beams strengthened with CFRP plate. The objective of the present investigation is to improve the method developed by Tounsi (2008) by assuming a parabolic shear stress across the depth of both CFRP plate and damaged RC beams. The objectives of this paper are first to present an improvement to Tounsi's solution (2008) to obtain a new closed-form solution which accounts for the parabolic adherend shear deformation effect in both the beam and bonded plate and second to compare quantitatively its solution against the new one developed in this paper by numerical illustrations. Numerical examples and a parametric study are presented to illustrate the governing parameters that control the stress concentrations at the edge of the CFRP strip. Finally, the adopted improved model describes better the actual response of the CFRP- damaged RC hybrid beams and permits the evaluation of the adhesive stresses, the knowledge of which is very important in the design of such structures. It is believed that the present results will be of interest to civil and structural engineers and researchers. In the present research a finite element model was developed using the commercial code ABAQUS (2007) to evaluate the interfacial shear stress of damaged RC beam strengthened with a bonded GFRP plate. The effects of the material and geometry parameters on the interface stresses are considered and compared with that resulting from literature. The simple approximate closed-form solutions discussed in this paper provide a useful but simple tool for understanding the interfacial behaviour of an externally bonded FRP plate on the damaged concrete beam.

We can also mention, in addition to the composite fiber matrix materials, another alternative can be proposed to strengthen the structures that will be addressed in our future research, it is therefore the use of functionally graded materials (FGM) (Cheikh 2017, Tounsi 2013, Mahi 2015, Kaci 2018, Draiche 2016, Belabed 2018, Abdelha 2016, Abdelaziz 2017, Bennoun 2016) that in order to improve and ensure the material continuity through the thickness of the reinforcing plate, aiming as a parameter in the mechanical characteristics of FGM, all by passing laws adequately mixes to better meet industrial requirements and the environmental condition.

2. Finite element analysis

In comparison with laboratory tests which are highly time and cost demanding, the numerical simulation is cheaper, time-saving, not so dangerous and more information. As the computational power has intensely increased, numerical methods, in particular the finite element method (FEM), have also been resorted for analysis of many practical engineering problems. The modeling process in Abaqus consists of defining the various components of the model individually i.e., the reinforced concrete beam, CFRP plate and adhesive layer were defined as parts, each compatible with the other so as to provide a complete analysis. The modeling itself is an iterative process, in that it takes several analyses to be able to simulate a particular set of characteristics effectively. A 4-node linear quadrilateral, type S4R was established, in which only one half of the beam was considered because of symmetry geometry and loading of the beam (Fig. 1). All nodes at mid-span were restrained to produce the required symmetry, and nodes at the end of the RC beam were restrained to represent simply roll-supported conditions. The finite element mesh was refined in correspondence of the reinforcement ends in order to capture the relevant stress concentration with a total of C3D20R- 131150 elements for FRP-RC hybrid beam. The number of elements used depends largely on the geometric parameters such as the length and the cross-sectional perimeter. In order to obtain accurate stress results at the ends of the plate, a fine mesh was deployed in these areas, as shown in Fig. 1.

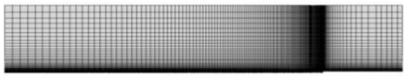

Fig. 1 Finite Element mesh of a half damaged RC beam strengthened with bonded CFRP plate model

The relevant geometrical and mechanical properties used in the finite element analysis were the same as that used in the analytical method shown in Table 1. To simulate correctly the interaction behavior between the various components of the composite beams, a surface-to-surface contact interaction describes contact between two deformable surfaces. Element types and material properties were then specified and assigned to each corresponding part. A single concentrated load was applied at the mid-span of the strengthened damaged RC beam. While the damaged RC beam was assigned isotropic material properties, unidirectional laminate stress-strain relationship was adopted for the CFRP plate and elastic material properties for the adhesive layer. In this work, the stresses have been obtained from the average values of the stress in the bottom elements of the adhesive layer.

3. Analytical analysis and solutions procedure

3.1 Assumptions of the solution

One of the analytical approach proposed by Hassaine Daouadji (2008) for concrete beam strengthened with a bonded GFRP Plate was used in order to compare it with a finite element analysis. The analytical approach (Hassaine Daouadji 2008) is based on the following assumptions:

- Bending deformations of the adhesive are neglected.
- No slip is allowed at the interface of the bond.
- All materials considered are linear elastic.
- The beam is simply supported and shallow, i.e., plane sections remain plane in bending.
- Stresses in the adhesive layer do not change with the thickness.

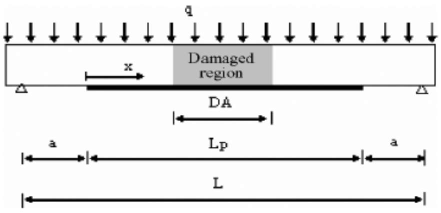

Fig. 2 Simply supported damaged RC beam strengthened with bonded GFRP plate

- The shear stress analysis assumes that the curvatures in the beam and plate are equal. However, this assumption is not made in the peel stress solution. When the beam is loaded, vertical separation occurs between RC beam and GFRP plate. This separation creates an interfacial normal stress in the adhesive layer. We note that this assumption is used in several works, e.g., Tounsi (2006, 2008).
- A parabolic shear stress distribution through the depth of both the concrete beam and the bonded plate is assumed.
- The section properties of the damaged RC beam were based on the uncracked section, excluding the conventional steel reinforcement. It is known that for uncracked section, the concrete can sustain tension. However, for cracked section, the concrete cannot sustain tension and this is why the effect of steel reinforcement in concrete is not neglected.

3.2 Material properties of damaged plates:

The model's Mazars (1984, 1996) is based on elasticity coupled with isotropic damage and ignores any manifestation of plasticity, as well as the closing of cracks. This concept directly describes the loss of rigidity and the softening behavior. The constraint is determined by the following relation

$$\sigma_{ij} = (1-\varphi)C_{ijkl}\varepsilon_{kl} \qquad 0 < \varphi < 1 \tag{1a}$$

$$\tilde{E}_{11} = E_{11}(1-\varphi) \tag{1b}$$

$$\tilde{E}_{22} = E_{22}(1-\varphi) \tag{1c}$$

where $\tilde{E}_{11}$, $\tilde{E}_{22}$ and E_{11}, E_{22} are the elastic constants of damaged and undamaged state, respectively, and φ is damaged variable. Hence, the material properties of the damaged plate can be represented by replacing the above elastic constants with the effective ones defined in Eq. (1b) and (1c).

3.3 Basic equation of elasticity:

Fig. 2 shows a schematic sketch of the steps involved in strengthening a damaged RC beam with a bonded GFRP plate. A differential section, dx, can be cutout from the GFRP- strengthened damaged RC beam, as shown in Fig. 3. The strains in the RC beam near the adhesive interface and the external FRP reinforcement can be expressed, respectively as

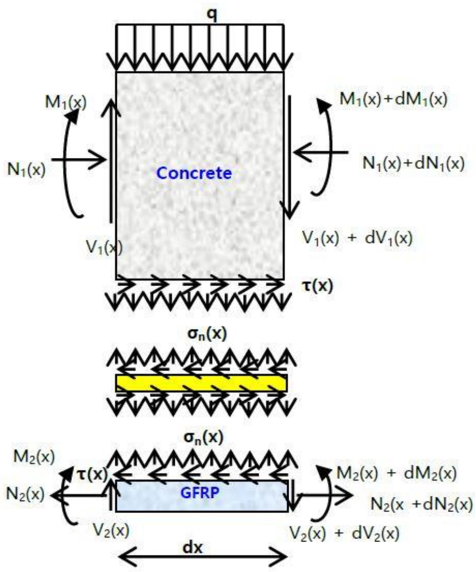

Fig. 3 Forces in infinitesimal element of a soffit-plated

$$\varepsilon_1(x) = \frac{du_1(x)}{dx} = \frac{y_1}{E_1 I_1} M_1(x) + \frac{N_1(x)}{E_1 A_1} \tag{2}$$

$$\varepsilon_2(x) = \frac{du_2(x)}{dx} = \frac{-y_2}{E_2 I_2} M_2(x) + \frac{N_2(x)}{E_2 A_2} - \frac{5t_2}{12G_2}\frac{d\tau_a}{dx} \tag{3}$$

Where $N(x)$ is the axial force in each adherend and A is the cross sectional area. On the other hand, the laminate theory is used to determine the stress and strain of the externally bonded composite plate in order to investigate the whole mechanical performance of the composite strengthened structure. The effective modules of the composite laminate are varied by the orientation of the fibre directions and arrangements of the laminate patterns. The classical laminate theory is used to estimate the strain of the composite plate, i.e.

$$\begin{Bmatrix} \varepsilon^0 \\ k \end{Bmatrix} = \begin{bmatrix} A' & B' \\ C' & D' \end{bmatrix} \begin{Bmatrix} N \\ M \end{Bmatrix} \tag{4}$$

$$\begin{aligned} [A'] &= [A]^{-1} + [A]^{-1}[B][D^*]^{-1}[B][A]^{-1} \\ [B'] &= -[A]^{-1}[B\ ][D^*]^{-1} \\ [C'] &= [B']^T \\ [D'] &= [D^*]^{-1} \\ [D^*] &= [D] - [B][A]^{-1}[B] \end{aligned} \tag{5}$$

The terms of the matrices $[A]$, $[B]$ and $[D]$ are written as:

Extensional matrix:

$$A_{ij} = \sum_{k=1}^{NN} \overline{Q}_{ij}^{k}((y_2)_k - (y_2)_{k-1}) \tag{6}$$

Extensional -bending coupled matrix:

$$B_{ij} = \frac{1}{2}\sum_{k=1}^{NN} \overline{Q}_{ij}^{k}((y_2^2)_k - (y_2^2)_{k-1}) \tag{7}$$

Flexural matrix:

$$D_{ij} = \frac{1}{3}\sum_{k=1}^{NN} \overline{Q}_{ij}^{k}\left((y_2^3)_k - (y_2^3)_{k-1}\right) \quad (8)$$

The subscript NN represents the number of laminate layers of the GFRP plate, $\overline{Q}_{ij}$ can be estimated by using the off-axis orthotropic plate theory, where

$$\overline{Q}_{11} = Q_{11} m^4 + 2(Q_{12} + 2Q_{33})m^2n^2 + Q_{22}n^4 \quad (9)$$

$$\overline{Q}_{12} = (Q_{11} + Q_{22} - 4Q_{33})m^2n^2 + Q_{12}(n^4 + m^4) \quad (10)$$

$$\overline{Q}_{22} = Q_{11} n^4 + 2(Q_{12} + 2Q_{33})m^2n^2 + Q_{22}m^4 \quad (11)$$

$$\overline{Q}_{33} = (Q_{11} + Q_{22} - 2Q_{12} - 2Q_{33})m^2n^2 + Q_{33}(n^4 + m^4) \quad (12)$$

And

$$Q_{11} = \frac{E_1}{1 - \upsilon_{12}\upsilon_{21}} \quad (13)$$

$$Q_{22} = \frac{E_2}{1 - \upsilon_{12}\upsilon_{21}} \quad (14)$$

$$Q_{12} = \frac{\upsilon_{12}E_2}{1 - \upsilon_{12}\upsilon_{21}} = \frac{\upsilon_{21}E_1}{1 - \upsilon_{12}\upsilon_{21}} \quad (15)$$

$$Q_{33} = G_{12} \quad (16)$$

$$m = \cos(\theta_j) \; n = \sin(\theta_j) \quad (17)$$

Where j is number of the layer; h, $\overline{Q}_{ij}$ and θ_j are respectively the thickness, the Hooke's elastic tensor and the fibers orientation of each layer.

Assume that the ply arrangement of the plate is symmetrical with respect to the mid-plane axis $y_2 = 0$. A great simplification in laminate analysis then occurs by assuming that the coupling matrix B is identically zero. Therefore Eqs. (4)-(8) can be simplified to the following matrix form for a plate with a width of b_2

$$\{\varepsilon^0\} = [A']\{N\}_2 \quad \text{and} \quad \{k\} = [D']\{M\}_2 \quad (18)$$

Where: $$\{\varepsilon^0\}_2 = \begin{Bmatrix} \varepsilon_x^0 \\ \varepsilon_y^0 \\ \gamma_{xy}^0 \end{Bmatrix}, \quad \{k\}_2 = \begin{Bmatrix} k_x \\ k_y \\ k_{xy} \end{Bmatrix} \quad (18a)$$

$$\{N\}_2 = \begin{Bmatrix} N_x \\ N_y \\ N_{xy} \end{Bmatrix}_2, \quad \{M\}_2 = \begin{Bmatrix} M_x \\ M_y \\ M_{xy} \end{Bmatrix}_2 \quad (18b)$$

In the present study, only an axial load N_x and the bending moment M_x in the beam's longitudinal axis are considered, i.e., $N_y = N_{xy} = 0$ and $M_y = M_{xy} = 0$. Therefore, Eq. 4 can be simplified to

$$\varepsilon_x^0 = \frac{A_{11}^{'} N_x}{b_2} \quad \text{and} \quad k_x = \frac{D_{11}^{'} M_x}{b_2} \quad (19)$$

Using CLT, the strain at the top of the GFRP plate 2 is given as

$$\varepsilon_2(x) = \varepsilon_x^0 - k_x \frac{t_2}{2} \quad (20)$$

Substituting equation, gives the following equation

$$\varepsilon_2(x) = \frac{du_2(x)}{dx} = -D_{11}^{'} \frac{t_2}{2b_2} M(x) + A_{11}^{'} \frac{N_2(x)}{b_2} \quad (21)$$

Where: $N_2(x) = N$, and $M_2(x) = M_x$

The subscripts 1 and 2 denote adherends 1 and 2, respectively. $M(x)$, $N(x)$ and $V(x)$ are the bending moment, axial and shear forces in each adherend.

3.4 Mathematical formulation of shear stress distribution along the GFRP-damaged RC interface

The governing differential equation for the interfacial shear stress (Rabahi 2016) is expressed as:

$$\frac{d^2\tau(x)}{dx^2} - K_1\left(A_{11}^{'} + \frac{b_2}{E_1A_1} + \frac{(y_1 + t_2/2)(y_1 + t_a + t_2/2)}{E_1I_1D_{11}^{'} + b_2} b_2 D_{11}^{'}\right) \tau(x) + K_1\left(\frac{(y_1 + t_2/2)}{E_1I_1D_{11}^{'} + b_2} D_{11}^{'}\right) V_T(x) = 0 \quad (22)$$

Where

$$K_1 = \frac{1}{\left(\dfrac{t_a}{G_a} + \dfrac{5t_2}{12G_2}\right)} \quad (23)$$

For simplicity, the general solutions presented below are limited to loading which is either concentrated or uniformly distributed over part or the whole span of the beam, or both. For such loading, $d^2V_T(x)/dx^2 = 0$, and the general solution to Eq. (22) is given by

$$\tau(x) = B_1\cosh(\lambda x) + B_2\sinh(\lambda x) + m_1 V_T(x) \quad (24)$$

Where

$$\lambda^2 = K_1\left(A_{11}^{'} + \frac{b_2}{E_1A_1} + \frac{(y_1 + t_2/2)(y_1 + t_a + t_2/2)}{E_1I_1D_{11}^{'} + b_2} b_2 D_{11}^{'}\right) \quad (25)$$

And

$$m_1 = \frac{K_1}{\lambda^2}\left(\frac{(y_1 + t_2/2)}{E_1I_1D_{11}^{'} + b_2} D_{11}^{'}\right) \quad (26)$$

And B_1 and B_2 are constant coefficients determined from the boundary conditions.

3.4 Application of boundary conditions:

The same loads cases used by Smith and Teng (2001) are considered in the present method. A simply supported beam is investigated which is subjected to a uniformly distributed load and an arbitrarily positioned single point load as shown in Fig. 4. This section derives the expressions of the interfacial shear stresses for each load case by applying suitable boundary conditions.

Interfacial shear stress for a uniformly distributed load: As is described by Smith and Teng (2001) the interfacial shear stress for this load case at any point is written as. The constants of integration need to be determined by applying

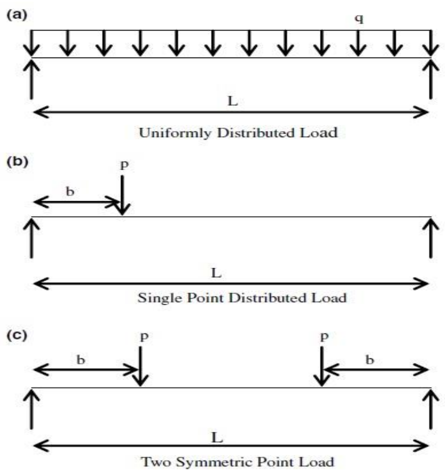

Fig. 4 Load cases

suitable boundary conditions. The first boundary condition is applied at the bending moment at x=0. Here, the moment at the plate end M_f (0) and the axial force of either the concrete beam or GFRP plate are zero. As a result, the moment in the section at the plate curtailment is resisted by the beam alone and can be expressed as

$$M_b(0) = M_t(0) = \frac{qa}{2}(L-a) \tag{27}$$

Applying the above boundary condition in Eq. (22)

$$\frac{d\tau(x=0)}{dx} = -m_2\, M_T(0)$$
$$m_2 = \frac{G_a}{t_a}\left(\frac{e}{E_b\, I_b} + \frac{\alpha\, T_b}{M_T(0)}\right) \tag{28}$$

By substituting equation, B2 can be determined as

$$B_2 = -\frac{q\, a\, m_2}{2\lambda}(L-a) + \frac{m_1}{\lambda}q \tag{29}$$

The second boundary condition requires zero interfacial shear stress at mid-span due to symmetry of the applied load. B1 can therefore be determined as

$$B_1 = \frac{a\, q\, m_2}{2\lambda}(L-a)\tanh\left(\frac{\lambda L_p}{2}\right) - \frac{q\, m_1}{\lambda}\tanh\left(\frac{\lambda\, L_p}{2}\right) \tag{30}$$

For practical cases $\frac{\lambda L_p}{2} \succ 10$ and as a result $\tanh\frac{\lambda L_p}{2} \approx 1$. So the expression for B_1 can be simplified to

$$B_1 = \frac{a\, q\, m_2}{2\lambda}(L-a) - \frac{q\, m_1}{\lambda} = -B_2 \tag{31}$$

Substitution of B_1 and B_2 into Eq. (24) gives an expression for the interfacial shear stress at any point

$$\tau(x) = \left[\frac{m_2 a}{2}(L-a) - m_1\right]\frac{qe^{-\lambda x}}{\lambda} + m_1 q\left(\frac{L}{2} - a - x\right) \qquad 0 \le \mathrm{x} \le \mathrm{L_P} \tag{32}$$

$$m_2 = K_1\left(\frac{e}{E_1 I_1} + \frac{\alpha\, T_b}{M_T(0)}\right) \tag{33}$$

where q is the uniformly distributed load (Fig. 4(a)) and x, a, L and L_p are defined in Fig. 1. Contrary, to the method presented by Smith and Teng (2001), the expression of m_2 in the present method which take into account the shear deformations of adherends become

Interfacial shear stress for a single point load: The general solution for the interfacial shear stress for this load case is

$a < b:$

$$\tau(x) = \begin{cases} \frac{m_2}{\lambda}Pa\left(1-\frac{b}{L}\right)e^{-\lambda x}\frac{q}{\lambda} + m_1 P\left(1-\frac{b}{L}\right) - m_1 P\cosh(\lambda x)e^{-k} & 0 \le x \le (\mathrm{b-a}) \\ \frac{m_2}{\lambda}Pa\left(1-\frac{b}{L}\right)e^{-\lambda x}\frac{q}{\lambda} - m_1\frac{Pb}{L} + m_1 P\sinh(k)e^{-\lambda x} & (\mathrm{b-a}) \le x \le \mathrm{L}p \end{cases} \tag{34}$$

$a > b:$

$$\tau(x) = \frac{m_2}{\lambda}Pb\left(1-\frac{a}{L}\right)e^{-\lambda x} - m_1\frac{Pb}{L} \qquad 0 \le \mathrm{x} \le \mathrm{Lp} \tag{35}$$

where P is the concentrated load (Fig. 4(b)) and k=λ(b−a). The expression of m_1, m_2 and, takes into consideration the shear deformation of adherends.

Interfacial shear stress for two point loads: The general solution for the interfacial shear stress for this load (Fig. 4(c)) case is

$a < b:$

$$\tau(x) = \begin{cases} \frac{m_2}{\lambda}Pae^{-\lambda x} + m_1 P - m_1 P\cosh(\lambda x)e^{-k} & 0 \le x \le (\mathrm{b-a}) \\ \frac{m_2}{\lambda}Pae^{-\lambda x} + m_1 P\sinh(k)e^{-\lambda x} & (\mathrm{b-a}) \le x \le \frac{\mathrm{L}p}{2} \end{cases} \tag{36}$$

$a > b:$

$$\tau(x) = \frac{m_2}{\lambda}Pbe^{-\lambda x} \qquad 0 \le \mathrm{x} \le \mathrm{Lp} \tag{37}$$

4. Results and discussions

Material used:

The material used for the present studies is an RC beam bonded with a glass fibre reinforced plastic GFRP. The beams are simply supported and subjected to a uniformly distributed load. A summary of the geometric and material properties is given in Table1. The span of the RC beam is 3000 mm, the distance from the support to the end of the plate is 300 mm .

Comparison with experimental results:

Table 1 Geometric and material properties

Component	Width (mm)	Depth (mm)	Young's modulus (MPa)	Poisson's ratio	Shear modulus (MPa)
RC beam	b_1=200	t_1=300	E_1=30 000	0.18	-
Adhesive layer	b_a=200	t_a= 4	E_a=3000	0.35	-
GFRP plate	b_2=200	t_2= 4	E_2=50 000	0.28	G_{12}=5000
Aluminum	b_2=200	t_2= 2	E_2=63500	0.30	

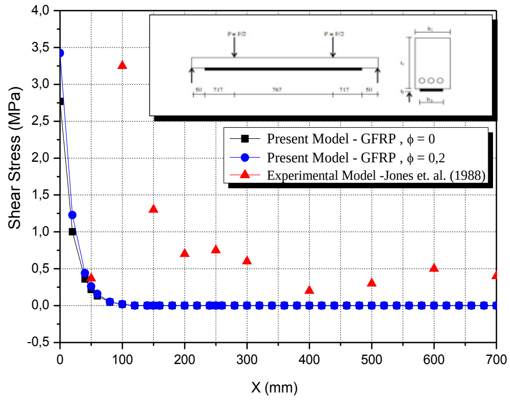

Fig. 5 Comparison of interfacial shear of the steel plated RC beam with the experimental results

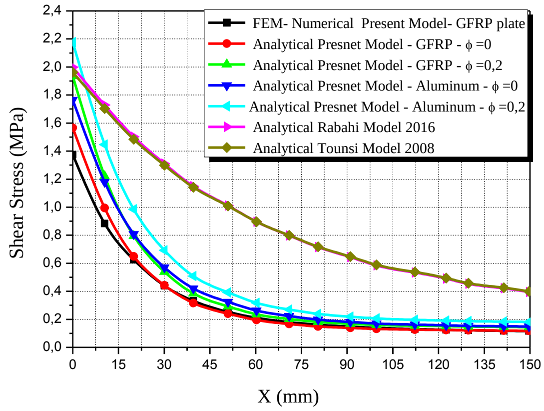

Fig. 6 Comparison of shear interfacial stress in damaged RC beam bonded with GFRP plate

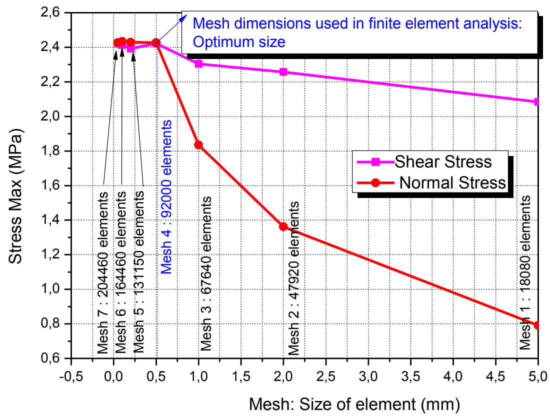

Fig. 7 Influence of element size in the direction on maximum shear stress at cutoff point

To validate the present method, a rectangular section is used here. One of the tested beams bonded with steel plate by Jones (1988), is analysed here using the present improved solution. The beam is simply supported and subjected to four-point bending, each at the third point. The geometry and materials properties of the specimen are summarized in the Table 1. The interfacial shear stress distributions in the beam bonded with a soffit steel plate under the applied load 180 kN, are compared between the experimental results and those obtained by the present model (damaged RC beam bonded by GFRP plate φ=0 and φ=0,2). As it can be seen from Fig. 5, the predicted analytical results are in reasonable agreement with the experimental results.

Comparison with analytical solutions: A comparison of the interfacial shear and normal stresses from the different existing closed-form solutions and the present new solution is undertaken in this section. An undamaged RC beam bonded with a GFRP soffit plate is considered. The beam is simply supported and subjected to to a different type of loading (uniformly distributed load, a single point distributed load and a Two symmetric point load) (Table 2). Fig. 6 plots the interfacial shear stress near the plate end for the example RC beam bonded with a GFRP plate for the uniformly distributed load case. Overall, the predictions of the different solutions agree closely with each other. As it can be seen from the results, the peak interfacial stresses assessed by the present theory are smaller compared to those given by Tounsi (2008), Rabahi (2016) solution. This implies that adherend shear deformation is an important factor influencing the adhesive interfacial shear stress distribution. Hence, it is apparent that the adherend shear deformation reduces the interfacial shear stress concentration and thus renders the adhesive shear distribution more uniform.

Comparison with numerical model: One of advantages of FEM simulation is that the detailed distributions of the shear stress along the interfaces can be produced. A simply supported damaged RC beam strengthened with a bonded CFRP plate. Taking advantage of the symmetry of the specimens, only one quarter of the beams was modelled, The influence of the mesh size on the predicted shear stress at the cutoff points was noticeable. In general, increasing the size of the elements results in a proportional increase in the distances among the integration points within the element. Therefore, the induced shear stresses at the strip cutoff points are averaged over a large distance and are considerably less than the true values. Decreasing the size of the elements results in a substantial increase in the maximum shear stress up to a certain limit beyond which no further increase in the shear stresses is observed. The size of the elements at this transition stage is termed the optimum size.The optimum size of the elements in the longitudinal as well as in the vertical directions was determined as shown in Fig. 7. Further refinement of the mesh around the cutoff points increased the predicted shear stress by less than 0.5 percent. The final mesh dimensions used for 92000 elements (mesh 4). The FEM solutions are compared with the present analytical model and the interfacial shear stress distributions near the end of FRP are shown in Fig. 6. The FEM results are in reasonable agreement with the analytical results.

Parametric studies: The parametric study program was based on FE analysis work and analytically approach, which will help engineers in optimizing their design parameters, the effects of several parameters were investigated.

Effect of plate stiffness on interfacial stress: Fig. 6 and Table 2, gives interfacial shear stresses for the damaged RC

Table 2 Comparison of interfacial shear stress (MPa)

Model	Effect of damage	RC beam with GFRP plate: Single Point Distributed Load	RC beam with GFRP plate: Two Symmetric Point Load	RC beam with GFRP plate: Uniformly Distributed Load	RC beam with Aluminum plate: Single Point Distributed Load	RC beam with Aluminum plate: Two Symmetric Point Load	RC beam with Aluminum plate: Uniformly Distributed Load
Comparison of interfacial shear stress (MPa): Perfect concrete (α=0%)							
Present	φ=0	2.459	2.767	1.565	2.767	3.090	1.765
Present	φ=0,1	2.719	3.060	1.731	3.056	3.415	1.949
Present	φ=0,2	3.040	3.423	1.935	3.412	3.814	2.176
Present	φ=0,3	3.448	3.884	2.194	3.862	4.320	2.463
Rabahi (2016)	φ=0	1.367	1.456	0.884	1.547	1.627	1.004
Tounsi (2008)	φ=0	1.341	1.426	0.868	1.518	1.592	0.986
Comparison of interfacial shear stress (MPa): Imperfect concrete (α=2%)							
Present	φ=0	2.507	2.821	1.596	2.820	3.150	1.799
Present	φ=0,1	2.772	3.120	1.764	3.114	3.480	1.986
Present	φ=0,2	3.099	3.489	1.972	3.476	3.887	2.217
Present	φ=0,3	3.514	3.959	2.236	3.935	4.402	2.509
Rabahi (2016)	φ=0	1.384	1.473	0.895	1.566	1.645	1.016
Tounsi (2008)	φ=0	1.358	1.443	0.879	1.537	1.611	0.998
Comparison of interfacial shear stress (MPa): Imperfect concrete (α=4%)							
Present	φ=0	2.557	2.877	1.627	2.875	3.212	1.834
Present	φ=0,1	2.827	3.182	1.799	3.175	3.548	2.025
Present	φ=0,2	3.160	3.558	2.011	3.544	3.963	2.260
Present	φ=0,3	3.583	4.036	2.280	4.010	4.487	2.557
Rabahi (2016)	φ=0	1.401	1.491	0.907	1.585	1.664	1.029
Tounsi (2008)	φ=0	1.376	1.460	0.891	1.557	1.630	1.011

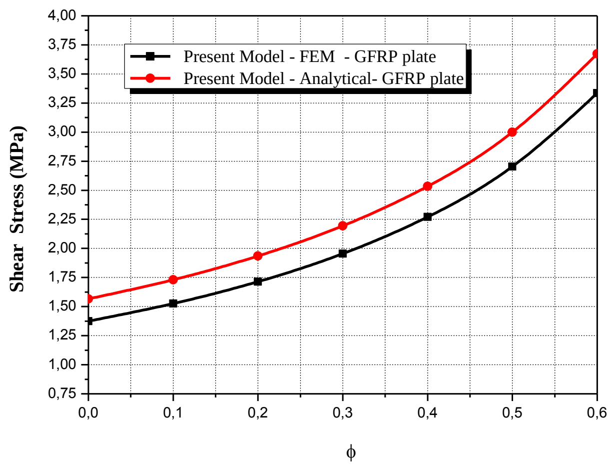

Fig. 8 Effects of damage on the maximal interfacial shear stress of RC beam strengthened by a GFRP plate

beam bonded with a GFRP plate and Aluminum plate, respectively, which demonstrates the effect of plate material properties on interfacial stresses. The length of the plate is Lp=2400 mm, and the thickness of the plate and the adhesive layer are both 4 mm. The results show that, as the plate material becomes softer (from aluminum to GFRP), the interfacial stresses become smaller, as expected. This is because, under the same load, the tensile force developed in the plate is smaller, which leads to reduced interfacial stresses. The position of the peak interfacial shear stress moves closer to the free edge as the plate becomes less stiff.

Effect of damaged on the maximal interfacial shear stresses: Fig. 8 show the effect of damage extent on maximum shear interfacial stress, for the GFRP materials. The results show that when the damage variable φ increases from 0 to 0.15, the maximum interfacial stress increase slowly. However, it can be seen that from 0.20 to 0.60, these stresses increase rapidly.

Effect of length of unstrengthened region "a": The influence of the length of the ordinary-beam region (the region between the support and the end of the composite strip on the edge stresses) appears in Table 3. It is seen that, as the plate terminates further away from the supports, the interfacial shear stress increase significantly. This result reveals that in any case of strengthening, including cases where retrofitting is required in a limited zone of maximum bending moments at midspan, it is recommended to extend the strengthening strip as possible to the lines.

Table 3 Effect of length of unstrengthened region "*a*" of damaged RC beam bonded with a GFRP plate subjected to a uniformly distributed load

	Effect of damage	a=50	a=100	a=150	a=200	a=250	a=300
Shear stress	φ=0	0,5241	0,8841	1,2313	1,5657	1,8873	2,1961
	φ=0,1	0,5789	0,977	1,3612	1,7311	2,0868	2,4283
	φ=0,2	0,6466	1,092	1,5217	1,9355	2,3334	2,7155
	φ=0,3	0,7322	1,237	1,7253	2,1948	2,6464	3,0799

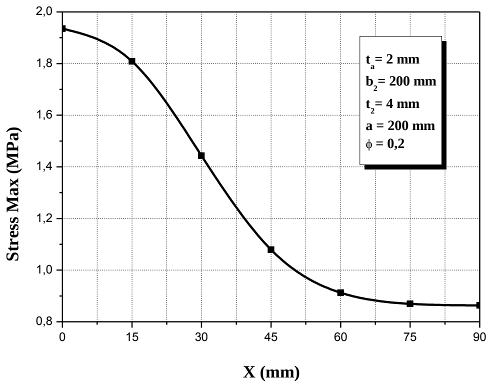

Fig. 9 Effects of fiber orientation on the maximal interfacial shear stress of RC beam strengthened by a GFRP plate

Effect of fiber orientation: The effect of fiber orientation on adhesive stresses is show in figure 9, the maximum interfacial shear stress increase with increasing alignment of all high strength fibers in the composite plate in beam's longitudinal direction x.

Effect of adhesive layer thickness:

Table 4 shows the effects of the thickness of the adhesive layer on the interfacial shear stress. Increasing the thickness of the adhesive layer leads to a significant reduction in the peak interfacial stresses. Thus using thick adhesive layer, especially in the vicinity of the edge, is recommended. In addition, it can be shown that these stresses decrease during time, until they become almost constant after a very long time.

5. Conclusions

This paper has been concerned with the prediction of interfacial shear stress in damaged RC beams retrofitted with externally advanced composite materials, were investigated by analytical and the finite element method and subjected to a uniformly distributed bending load. Such interfacial stresses provide the basis for understanding debonding failures in such beams and for development of suitable design rules. Numerical comparison between the existing solutions and the present new solution has been carried out. The results show that the damage has a significant effect on the interfacial stresses in GFRP-damaged RC beam, especially, when the length of damaged region is equal or superior to the plate length. The numerical examples show that the FE calculations are in good agreements with the theoretical analysis.

Table 4 Effect of adhesive layer thickness of damaged RC beam bonded with a GRP plate subjected to a uniformly distributed load

	Effect of damage	t_a=1	t_a=2	t_a=3	t_a=4	t_a=5	t_a=6
Shear stress	φ=0	2,0189	1,5657	1,3335	1,1863	1,0824	1,0039
	φ=0,1	2,2323	1,7311	1,4742	1,3114	1,1964	1,1096
	φ=0,2	2,4963	1,9355	1,6481	1,4660	1,3373	1,2402
	φ=0,3	2,8312	2,1948	1,8686	1,6619	1,5159	1,4057

Consequently, it is recommended to use a strengthening plate having length, superior to the damaged zone. The results reveal also, that thickness of the GFRP strip significantly increases the edge peeling and shear stresses. Observations were made based on the numerical results concerning their possible implications to practical designs. we can conclude that, This research is helpful for the understanding on mechanical behavior of the interface and design of the GFRP-RC hybrid structures.

In conclusion, we can say that in addition to matrix composite fiber materials, another alternative may be proposed for strengthening structures. This will involve the use of functionally graded materials (FGM) (Bouafi 2007, Bellifa 2017, Elhaina 2017, Menasria 2017, Adim 2016, Benferhat 2016, Attia 2018, Abualnour 2018, Benchora 2018, Tounsi 2013) in order to ensure continuity properties lift through the thickness of the reinforcement plate.

Acknowledgments

This research was supported by the French Ministry of Foreign Affairs and International Development (MAEDI) and Ministry of National Education, Higher Education and Research (MENESR) and by the Algerian Ministry of Higher Education and Scientific Research (MESRS) under Grant No. PHC Tassili 17MDU992. Their support is greatly appreciated.

References

Abaqus Guide Version 6.7 (2007), Computer Software for Interactive Finite Element Analysis by Hibbitt, Karlsson & Sorensen, Inc., Pawtucket, RI.

Abdelaziz, H.H., Meziane, M.A.A., Bousahla, A.A., Tounsi, A., Mahmoud, S.R. and Alwabli, A.S. (2017), "An efficient hyperbolic shear deformation theory for bending, buckling and free vibration of FGM sandwich plates with various boundary conditions", *Steel Compos. Struct.*, **25**(6), 693-704.

Abdelhak, Z., Hadji, L., Hassaine Daouadji, T. and Adda, B. (2016), "Thermal buckling response of functionally graded sandwich plates with clamped boundary conditions", *Smart Struct. Syst.*, **18**(2), 267-291.

Abualnour, M., Houari, M.S.A., Tounsi, A. and Mahmoud, S.R. (2018), "A novel quasi-3D trigonometric plate theory for free vibration analysis of advanced composite plates", *Compos. Struct.*, **184**, 688-697.

Adim, B., Hassaine Daouadji, T., Abbes, B. and Rabahi, A. (2016), "Buckling and free vibration analysis of laminated composite plates using an efficient and simple higher order shear deformation theory", *J. Mech. Industry*, **17**(5), 512.

Al-Emrani, M. and Kliger, R. (2006), "Analysis of interfacial shear stresses in beams strengthened with bonded prestressed laminates", *Compos. Part B: Eng.*, **37**(4-5), 265-272.

Ashraful, A. and Al Riyami, R. (2018), "Shear strengthening of reinforced concrete beam using natural fibre reinforced polymer laminates", *Constr. Build. Mater.*, **162**, 683-696.

Attia, A., Bousahla, A.A., Tounsi, A., Mahmoud, S.R. and Alwabli, A.S. (2018), "A refined four variable plate theory for thermoelastic analysis of FGM plates resting on variable elastic foundations", *Struct. Eng. Mech.*, **65**(4), 453-464.

Belabed, Z., Bousahla, A.A., Houari, M.S.A., Tounsi, A. and Mahmoud, S.R. (2018), "A new 3- unknown hyperbolic shear deformation theory for vibration of functionally graded sandwich plate", *Earthq. Struct.*, **14**(2), 103-115.

Bellifa, H., Bakora, A., Tounsi, A., Bousahla, A.A. and Mahmoud, S.R. (2017), "An efficient and simple four variable refined plate theory for buckling analysis of functionally graded plates", *Steel Compos. Struct*., **25**(3), 257-270.

Benferhat, R., Hassaine Daouadji, T. and Mansour, M.S. (2016), "Free vibration analysis of FG plates resting on the elastic foundation and based on the neutral surface concept using higher order shear deformation theory", *Comptes Rendus Mecanique*, **344**(9), 631-641 .

Bennoun, M., Houari, M.S.A. and Tounsi, A. (2016), "A novel five variable refined plate theory for vibration analysis of functionally graded sandwich plates", *Mech. Adv. Mater. Struct.*, **23**(4), 423-431.

Benyoucef, S., Tounsi, A., Meftah, S.A. and Adda Bedia, E.A. (2006), "Approximate analysis of the interfacial stress concentrations in FRP-RC hybrid beams", *Compos. Interf.*, **13**(7), 561-571.

Bouafia, K., Kaci, A., Houari, M.S.A., Benzair, A. and Tounsi, A. (2017), "A nonlocal quasi-3D theory for bending and free flexural vibration behaviors of functionally graded nanobeams", *Smart Struct. Syst.*, **19**(2), 115-126.

Bouakaz, K., Hassaine Daouadji, T., Meftah, S.A., Ameur, M., Tounsi, A. and Bedia, E.A. (2014), "A Numerical analysis of steel beams strengthened with composite materials", *Mech. Compos. Mater.*, **50**(4), 685-696.

Chen, W., Pham, T.M., Sichembe, H., Chen, L. and Hao, H. (2018), "Experimental study of flexural behaviour of RC beams strengthened by longitudinal and U-shaped basalt FRP sheet", *Compos. Part B: Eng.*, **134**, 114-126

Chikh, A., Tounsi, A., Hebali, H. and Mahmoud, S.R. (2017), "Thermal buckling analysis of cross-ply laminated plates using a simplified HSDT", *Smart Struct. Syst.*, **19**(3), 289-297.

Hassaine Daouadji, T., Rabahi, A., Abbes, B. and Adim, B. (2016), "Theoretical and finite element studies of interfacial stresses in reinforced concrete beams strengthened by externally FRP laminates plate", *J. Adhes. Sci. Technol.*, **30**(12), 1253-1280.

Draiche, K., Tounsi, A. and Mahmoud, S.R. (2016), "A refined theory with stretching effect for the flexure analysis of laminated composite plates", *Geomech. Eng.*, **11**(5), 671-690.

El-Haina, F., Bakora, A., Bousahla, A.A., Tounsi, A. and Mahmoud, S.R. (2017), "A simple analytical approach for thermal buckling of thick functionally graded sandwich plates", *Struct. Eng. Mech*., **63**(5), 585-595.

Fu, B., Teng, J.G., Chen, G.M., Chen, J.F. and Guo, Y.C. (2018), "Effect of load distribution on IC debonding in FRP-strengthened RC beams: Full-scale experiments", *Compos. Struct.*, **188**, 483-496.

Guenaneche, B. and Tounsi, A. (2014), "Effect of shear deformation on interfacial stress analysis in plated beams under arbitrary loading", *Adhes. Adhesiv.*, **48**, 1-13.

Jadooe, A., Al-Mahaidi, R. and Abdouka, K. (2018), "Performance of heat-damaged partially-insulated RC beams strengthened with NSM CFRP strips and epoxy adhesive", *Constr. Build. Mater.*, **159**, 617-634.

Jones, R., Swamy, R.N. and Charif, A. (1988), "Plate separation and anchorage of reinforced concrete beams strengthened by epoxy-bonded steel plates", *Struct. Eng.*, **66**(5), 85-94.

Kaci, A., Houari, M.S.A., Bousahla, A.A., Tounsi, A. and Mahmoud, S.R. (2018), "Post-buckling analysis of shear-deformable composite beams using a novel simple two-unknown beam theory", *Struct. Eng. Mech.*, **65**(5), 621-631.

Krour, B., Bernard, F. and Tounsi, A. (2014), "Fibers orientation optimization for concrete beam strengthened with a CFRP bonded plate: A coupled analytical-numerical investigation", *Eng. Struct.*, **56**, 218-227.

Mahi, A. and Tounsi, A. (2015), "A new hyperbolic shear deformation theory for bending and free vibration analysis of isotropic, functionally graded, sandwich and laminated composite plates", *Appl. Math. Model.*, **39**, 2489-2508.

Mahi, B.E., Benrahou, K.H., Belakhdar, K., Tounsi, A. and Bedia, E.A. (2014), "Effect of the tapered of the end of a FRP plate on the interfacial stresses in a strengthened beam used in civil engineering applications", *Mech. Compos. Mater.*, **50**(4), 465-474.

Mazars, J. (1984), "Application de la mécanique de l'endommagement au comportement non linéaire et à la rupture du béton de structure", Thèse de Doctorat d'état, Université Paris 6.

Mazars, J.G. and Pijaudier-Cabot, G. (1996), "From damage to fracture mechanics and conversely: a combined approach", *Int. J. Solid. Struct.*, **33**, 3327-3342.

Meier, U. (1995), "Strengthening of structures using carbon fibre/epoxy composites", *Constr. Build. Mater.*, **9**(6), 341-51.

Menasria, A., Bouhadra, A., Tounsi, A., Bousahla, A.A. and Mahmoud, S.R. (2017), "A new and simple HSDT for thermal stability analysis of FG sandwich plates", *Steel Compos. Struct.*, **25**(2), 157-175.

Mori, T. and Tanaka, K. (1973), "Average stress in matrix and average elastic energy of materials with misfitting inclusions", *Acta Metall*, **21**, 571-574.

Rabahi, A., Hassaine Daouadji, T., Abbes, B. and Adim, B. (2015), "Analytical and numerical solution of the interfacial stress in reinforced-concrete beams reinforced with bonded prestressed composite plate", *J. Reinf. Plast. Compos.*, **35**(3), 258-272.

Rabahi, A., Hassaine Daouadji, T., Benferhat, R. and Adim, B. (2018), "Elastic analysis of interfacial stress concentrations in CFRP-RC hybrid beams: Effect of creep and shrinkage", *Adv. Mater. Res.*, **6**(3), 257-278.

Roberts, T.M. (1989), "Approximate analysis of shear and normal stress concentrations in the adhesive layer of plated RC beams", *Struct. Eng*., **67**(12), 229-233.

Roberts, T.M. and Haji-Kazemi, H. (1989), "Theoretical study of the behavior of reinforced concrete beams strengthened by externally bonded steel plates", *Proc. Inst. Civil Eng*., **87**(Part2), 39-55

Shen, H.S., Teng, J.G. and Yang, J. (2001), "Interfacial stresses in beams and slabs bonded with thin plate", *J. Eng. Mech*., ASCE, **127**(4), 399-406.

Shen, K., Wan, S., Mo, Y.L. and Jiang, Z. (2018), "Theoretical analysis on full torsional behavior of RC beams strengthened with FRP materials", *Compos. Struct*., **183**, 347-357.

Smith, S.T. and Teng, J.G. (2001), "Interfacial stresses in plated beams", *Eng. Struct*., **23**(7), 857-871.

Thai, H.T. and Kim, S.E. (2018), "A new quasi-3D sinusoidal shear deformation theory for functionally graded plates", *Struct. Eng. Mech.*, **65**(1), 19-31.

Touati, M., Tounsi, A. and Benguediab, M. (2015), "Effect of shear deformation on adhesive stresses in plated concrete beams: Analytical solutions", *Comput. Concrete*, **15**(3), 141-166

Tounsi, A. (2006), “Improved theoretical solution for interfacial stresses in concrete beams strengthened with FRP plate”, *Int. J. Solid. Struct.*, **43**, 4154-4174.

Tounsi, A., Hassaine Daouadji, T., Benyoucef, S. and Adda bedia, E.A. (2008), “Interfacial stresses in FRP-plated RC beams: Effect of adherend shear deformations”, *Int. J. Adhes. Adhesiv.*, **29**(4), 343-351.

Tounsi, A., Houari, M.S.A. and Benyoucef, S. (2013), “A refined trigonometric shear deformation theory for thermoelastic bending of functionally graded sandwich plates”, *Aerosp. Sci. Technol*., **24**(1), 209-220.

Vilnay, O. (1988), “The analysis of reinforced concrete beams strengthened by epoxy bonded steel plates”, *Int. J. Cement Compos. Light Weight Concrete*, **10**(2), 73-78.

Wattanasakulpong, N. and Ungbhakorn, V. (2014), “Linear and nonlinear vibration analysis of elastically restrained ends FGM beams with porosities”, *Aerosp. Sci. Technol.*, **32**(1), 111-120.

Yang, J. and Wu, Y.F. (2007), “Interfacial stresses of FRP strengthened concrete beams: Effect of shear deformation”, *Compos. Struct.*, **80**, 343-351.

Yang, J. and Ye, J. (2010), “An improved closed-form solution to interfacial stresses in plated beams using a two-stage approach”, *Int. J. Mech. Sci.*, **52**, 13-30

Yang, J., Ye, J. and Niu, Z. (2007), “Interfacial shear stress in FRP-plated RC beams under symmetric loads”, *Cement Concrete Compos.*, **29**, 421-432

Yang, X., Gao, W.Y., Dai, J.G., Lu, Z.D. and Yu, K.Q. (2018), “Flexural strengthening of RC beams with CFRP grid-reinforced ECC matrix”, *Compos. Struct.*, **189**, 9-26.

Zidani, M.B., Belakhdar, K., Tounsi, A. and Adda Bedia, E.A. (2015), “Finite element analysis of initially damaged beams repaired with FRP plates”, *Compos. Struct.*, **134**, 429-439.

AT